

HARNESSING SURFACE WRINKLING TO MEASURE THE VISCOELASTIC PROPERTIES OF POLYMER FILMS AND COATINGS

Edwin P. Chan, Kirt A. Page, and Christopher M. Stafford
National Institute of Standards and Technology, Polymers Division
100 Bureau Drive
Gaithersburg, MD 20899

Presented at
THE WATERBORNE SYMPOSIUM
Advances in Sustainable Coatings Technology
February 10-12, 2010
New Orleans, LA, USA

Symposium Sponsored by
The University of Southern Mississippi
School of Polymers and High Performance Materials

ABSTRACT

To promote sustainable principles in films and coatings, reducing thickness offers one strategy for minimizing materials consumption. However, as the thickness of the polymer film reduces, its physical properties may be different compared to that of the bulk polymer. As the performance of the coating is dependent on the viscoelastic response of the polymer film, thus, it is necessary to directly measure the viscoelastic properties of the polymer thin film as these properties cannot be predicted based on bulk properties. While there are many measurement tools available for characterizing the viscoelastic properties of bulk polymers, only a limited number of techniques are capable of measuring the viscoelastic properties of polymer thin films. In this work, we present a new measurement technique based on surface wrinkling that can quantify the viscoelastic properties of polymer thin films. Our approach utilizes real-time laser-light scattering (SALS) to observe the kinetics of thermally-induced surface wrinkling, which evolves isothermally as a function of annealing time. Specifically, wrinkling is induced by applying a thermal stress to a sub-micron thick polymer film that is sandwiched between a rigid substrate and a thin superstrate. By following the time evolution of the wrinkle wavelength and amplitude with SALS, we can infer the elastic modulus and shear viscosity of the polymer film with the aid of a theoretical model. We demonstrate our approach by measuring the elastic modulus and shear viscosity of polystyrene (PS) films at annealing temperatures slightly above its glass transition temperature. For PS films with thicknesses considered as “bulk”, both the elastic modulus and shear viscosity are very comparable to the results measured by traditional shear rheometry. Interestingly, we observe a significant change in both the elastic modulus and shear viscosity for PS thin films compared with that of the “bulk” PS films.

Introduction

Minimizing materials consumption represents one possible strategy to promote sustainable principles in materials production and use. For polymer films and coatings, reducing the thickness of the layer offers such a strategy, which can be easily accomplished by changing the film processing conditions.

However, utilizing such a strategy must not compromise the mechanical properties of the film. As recent research has demonstrated, the mechanical properties of polymer films below a critical thickness can be significantly different compared to that of the bulk.^{1,2} Because most applications for polymer films have structural requirements, the mechanical properties of these materials must be carefully considered. An additional complexity for polymers is the fact that mechanical properties of most polymers are time- and/or temperature-dependent, i.e. viscoelastic.

There are well-established experimental approaches and theoretical models to characterize and predict the viscoelastic properties for bulk polymers. However, limited approaches are available to characterize the viscoelastic properties for polymer thin films. Hence, there is a need to develop measurement methods capable of quantifying the viscoelastic properties of polymer thin films.

In this contribution, we present a new measurement technique based on thermal wrinkling that can be utilized to quantify the viscoelastic properties of polymer thin films.³ Our measurement technique utilizes real-time laser-light scattering (SALS) to observe the kinetics of thermally-induced surface wrinkling, which evolves isothermally as a function of annealing time. Specifically, wrinkling is induced by generating a thermal-mismatch stress to a sub-micron thick polymer film that is confined by a rigid substrate and a thin superstrate. By following the time evolution of the wrinkle wavelength and amplitude with SALS, we can infer the elastic modulus and shear viscosity of the polymer film with the aid of a theoretical model.

Background

Mechanism of Thermal Wrinkling. Thermal wrinkling is a type of surface instability that occurs when a polymer thin film, sandwiched between stiffer inorganic substrate and superstrate layers, is heated to elevated temperatures (Figure 1). Due to the differences in thermal expansion coefficients (α) between the polymer and the stiffer layers ($\alpha_{polymer} > \alpha_{inorganic}$) and strain-compatibility condition at the interfaces, a net compressive stress develops at the polymer-superstrate interface when this composite layer is heated to elevated temperatures. At a critical temperature, a critical compressive stress (σ_w) leads to the development of surface wrinkles on the superstrate surface characterized by an isotropic morphology that can be approximated as a sinusoidal surface profile (Figure 1b) with defined wavelength and amplitude.

For a polymer with a primarily elastic mechanical response, application of a fixed compressive stress that is above the critical stress leads to the development of surface wrinkles whose wavelength and amplitude are stable over long times. For a polymer with a viscoelastic mechanical response, this constant critical compressive stress causes creep of the polymer film. As a result of the creep response, both the wavelength (d) and amplitude (A) of the surface wrinkles will evolve with time at a given temperature.

Relationship to Material Properties. From linear perturbation analysis, the amplitude change with time ($dA(t)/dt$) of the surface wrinkles for a viscoelastic polymer is described by the following:

$$\frac{dA(t)}{dt} = - \left[\frac{\frac{1-2\nu_i}{1-\nu_i} \left(\frac{h_i}{h_f} \right) \left(\frac{E_f}{12(1-\nu_f^2)} \left(\frac{2\pi h_f}{d(t)} \right)^4 - \sigma \left(\frac{2\pi h_f}{d(t)} \right)^2 \right) + \frac{E_i}{1+\nu_i}}{2\eta_i} \right] A(t) \quad (1)$$

The material constants of h_f , ν_f , E_f correspond to the film thickness, Poisson's ratio and elastic modulus of the aluminum layer, respectively. The material constants of h_i , ν_i , E_i , η_i correspond to the film thickness, Poisson's ratio, elastic modulus, and shear viscosity of the PS layer, respectively. This relationship is valid for a polymer film that is confined by both the superstrate and substrate, in other words, when the thickness of the polymer layer is commensurate with the thickness of the superstrate ($h_i/h_f < 10$).

Determination of the Rubbery Modulus. The material properties of elastic modulus and shear viscosity of the polymer film can be determined by simplification of eq. (1). At long times, the rate of change of the wrinkle amplitude reaches a plateau when A becomes commensurate with the superstrate film thickness due to the nonlinear effects of post-buckling deformation. Thus, $dA(t)/dt$ decreases and eventually reaches equilibrium when both A and d approaches a plateau ($A = A_r$, $d = d_r$).

For a glassy polymer film with a molecular mass above the entanglement limit, this plateau reflects the long-time limit, rubber-like state of the polymer characterized as a physically-entangled network of mobile polymer chains above its glass transition. The elastic modulus at the rubbery limit ($E_{i,r}$) is determined by using eq. (2) and applying the equilibrium condition of wrinkling, along with minimizing the elastic energy stored in polymer and superstrate layers, specifically, $dA(t)/dt = 0$ and $d\sigma/dk$ (where $k=2\pi/d$) = 0.

$$E_{i,r} = \frac{(1-2\nu_i)(1+\nu_i)}{12(1-\nu_i)} \left(\frac{E_f}{1-\nu_f^2} \right) \left(\frac{h_i}{h_f} \right) \left(\frac{2\pi h_f}{d_r} \right)^4 \quad (2)$$

Thus, the rubbery modulus of the polymer layer can be determined via thermal wrinkling simply by measuring the long time wavelength (d_r) of the surface wrinkles and prior knowledge of the materials properties of the polymer and superstrate layers.

Determination of the Shear Viscosity. The shear viscosity of the polymer film (η_i) can be determined at short times of the thermal wrinkling experiment when the rate of change of the wrinkle amplitude is the greatest. At the initial stages of the thermal wrinkling experiment, the initially flat film quickly evolves to a wrinkled surface whose amplitude change is characterized as an exponential growth. This exponential growth rate is captured in eq. (3):

$$\frac{dA(t)}{dt} = -S \cdot A(t) \quad (3)$$

and the growth rate exponent (S) is defined as:

$$S = \left[\frac{\frac{1-2\nu_i}{1-\nu_i} \left(\frac{h_i}{h_f} \right) \left(\frac{E_f}{12(1-\nu_f^2)} \left(\frac{2\pi h_f}{d(t)} \right)^4 - \sigma \left(\frac{2\pi h_f}{d(t)} \right)^2 \right) + \frac{E_i(t)}{1+\nu_i}}{2\eta_i} \right] \quad (4)$$

In addition to the materials properties, both the applied stress for wrinkling (σ) and the elastic modulus at early times ($E_i(t)$) must be known in order to determine η_i . The applied stress for wrinkling can be estimated based on the differences in thermal expansion coefficients between the respective layers, which will be discussed below. The elastic modulus at early times for the polymer layer is a function of the evolution of the wrinkle wavelength at early times ($d(t)$). Specifically, it is defined as:

$$E_i(t) = \frac{(1-2\nu_i)(1+\nu_i)}{12(1-\nu_i)} \left(\frac{E_f}{1-\nu_f^2} \right) \left(\frac{h_i}{h_f} \right) \left(\frac{2\pi h_f}{d(t)} \right)^4 \quad (5)$$

Materials and Experimental Approach. As we have discussed above, measurement of the isothermal wavelength and amplitude evolution of the surface wrinkles as a function of annealing time will allow for the interpolation of the viscoelastic properties of the polymer film. As a demonstration of the measurements of these materials properties, we use monodisperse polystyrene (PS) thin films with a molecular mass of 600,000 g/mole ($h_f = 270 \text{ nm} \pm 3 \text{ nm}$). These films are spin-coated onto silicon substrates, then annealed at elevated temperatures, and a thin layer of aluminum (Al) is thermally evaporated over the polymer films to generate the final composite films. These films are used directly for the thermal wrinkling experiments without additional processing.

To capture the dynamics of the wrinkle morphology in real-time, we adapt small-angle laser light scattering (SALS) to measure the changes in both the scattering pattern and intensity as a function of isothermal annealing time. Specifically, SALS was performed using a custom-built instrument (Figure 2). The composite film was placed on a hot stage (Linkam TMS94, Linkam Scientific Instruments^{††}), and held at predetermined annealing temperatures, typically 5-10 °C above the glass transition temperature of the polymer film. The 2-dimensional (2-d) scattering images were collected using a charge-coupled device (CCD) camera (Apogee kx260e, Apogee Instruments, Inc) with a time resolution of 0.5 s. The 2-d scattering pattern was radially averaged to determine the scattering intensity as a function of the scattering vector, k . The peak intensity was fitted as a Gaussian and the corresponding scattering vector was determined.

Representative time-resolved scattering images for PS that is thermally wrinkled at 125 °C are presented in Figures 2b and 2c. During early annealing times, the scattering profiles are featureless with relatively low intensity (Figure 2b). Because wrinkle formation is related to the thermal mismatch stress that develops within the composite film, we attribute this observation to the development of an applied stress below the critical value for wrinkle initiation.

As time progresses, the critical stress for wrinkling decreases due to changes in the viscoelastic properties of the PS layer. The constant applied stress is now significant enough to initiate the formation of surface wrinkles, which are characterized by an isotropic morphology of a dominant wavelength, d , and amplitude, A . This dominant wavelength is captured by SALS as the scattering vector, $k = (4\pi/\lambda)\sin\theta \approx 2\pi/d$. To a first-order approximation, the wrinkle amplitude is related to the peak intensity (I), and the wavelength of incident light (λ) as $A \approx I^{1/2}(\lambda/2\pi)$.

Results and Discussion

Rubbery Modulus and Shear Viscosity for PS. Figure 3 summarizes the change in d_r and S for a PS film ($h_i = 270 \text{ nm} \pm 3 \text{ nm}$, measured via interferometry), capped by an aluminum thin film ($h_f = 54 \text{ nm} \pm 1 \text{ nm}$, measured via atomic force microscopy), as a function of the thermal annealing temperature from 120 °C to 135 °C.

The rubbery modulus and shear viscosity for PS at a given annealing temperature can be determined by substituting the values of d_r and S , along with the defined materials constants into eq. (2) and eq. (4), respectively. The materials constants used are: $h_f = 54 \text{ nm}$, $\nu_f = 0.33$, $E_f = 7 \times 10^{10} \text{ N/m}^2$ for the Al thin film, and $h_i = 270 \text{ nm}$, $\nu_i = 0.495$ for the PS layer.

To determine the shear viscosity for PS, the applied stress for wrinkling must also be known. Specifically, the applied stress, σ , depends on the thermal history of the entire experiment, which includes residual stresses that develop within the layers during film processing and the thermal expansion-mismatch stress generated during the thermal wrinkling experiment. At the present, we can only estimate σ for our system by assuming that the residual stress is negligible and the entire contribution is associated with differences in thermal expansion. Previous works on thermal wrinkling of polymer films have suggested that the origin of the thermal-mismatch stress depends on the thickness of the polymer film.^{4,5} Specifically, the critical temperature for the development of surface wrinkles have been observed to increase as the film thickness decrease.

While questions remain over the specific mechanism of thermal wrinkling, we can establish upper and lower limits for the thermal-mismatch stress for wrinkling. If we assume that the origin of the thermal-mismatch stress is related to the differences in thermal expansion coefficients between the polymer layer (α_i) and superstrate thin film (α_f), then σ is defined as:⁶

$$\sigma \cong \frac{E_f}{1-\nu_f} \left[(\alpha_f - \alpha_{i,T>T_g})(T - T_g) + (\alpha_f - \alpha_{i,T<T_g})(T_g - T_{RT}) \right] \quad (6)$$

Because the glassy polymer undergoes a secondary phase transition at the glass transition temperature (T_g), the change in α for the polymer layer must be accounted for above and below the T_g . Eq. (6) predicts an upper limit of the applied stress because α for most polymers is at least an order of magnitude greater than most inorganic materials. With PS as the polymer layer ($\alpha_{i,T<T_g} = 5.7 \times 10^{-5} \text{ K}^{-1}$ and $\alpha_{i,T>T_g} = 1.7 \times 10^{-4} \text{ K}^{-1}$)⁷ and aluminum ($\alpha_f = 2.3 \times 10^{-5} \text{ K}^{-1}$)⁶ as the superstrate thin film, $\sigma \approx 7 \times 10^8 \text{ N/m}^2$ at 135 °C.

If we assume that the applied stress is related to the thermal expansion mismatch between the superstrate and substrate layers, then σ is independent of the polymer layer and a lower limit is estimated.⁷

$$\sigma \cong \frac{E_f}{1-\nu_f} (\alpha_f - \alpha_s) (T - T_{RT}) \quad (7)$$

For an aluminum superstrate and a silicon substrate ($\alpha_s = 5.5 \times 10^{-6} \text{ K}^{-1}$), $\sigma \approx 3 \times 10^8 \text{ N/m}^2$ at 135 °C. We choose this lower limit for the applied stress as this value is slightly below the yield stress for aluminum.

Comparison to Bulk Rheology. To demonstrate the accuracy of our technique, we compare our results with traditional parallel-plate rheometry. Specifically, we measured the rubbery modulus and shear viscosity of bulk PS using rheometry. The rubbery modulus and shear viscosity values from rheometry are compared with the values obtained from thermal wrinkling measurements (Figure 4).

Because the viscoelastic properties of PS are also strain-rate dependent, we compared the results from the two measurement techniques using similar strain rates. Although thermal wrinkling can be described as a creep measurement, i.e. a constant thermal-mismatch stress is applied over the course of the test, there exists a unique value of an average strain rate that is defined during the initial stage of the test as the temperature of the composite is increased from room temperature to the annealing temperature. We estimate the average strain rate ($\Delta\varepsilon/\Delta t$) in the thermal wrinkling experiments as the ratio of the change in wrinkle amplitude as a function of time versus the amplitude, which is coincidentally equivalent to the growth rate from eq. (4):

$$\frac{\Delta\varepsilon}{\Delta t} \approx \frac{dA(t)/A(t)}{dt} = S \quad (8)$$

The average strain rate, as approximated by S from Figure 3, increases with annealing temperature. Based on eq. (4), this result is expected since the applied stress increases with the annealing temperature. When we compare $E_{i,r}$ and η_i values at similar strain rates, the results from thermal wrinkling are in good agreement with bulk rheometry values (Figure 4).

There are slight deviations at the lower annealing temperature, which we attribute to the discrepancy in the strain rates for the techniques. While it is straightforward to define the strain rates in bulk rheometry, the strain rates for thermal wrinkling is controlled primarily by the rate of temperature increase from room temperature to the annealing temperature. Because $E_{i,r}$ from thermal wrinkling is measured at relatively long times, the estimated strain rates at these times are lower than the lowest rates used in bulk rheometry ($\sim 0.00001 \text{ s}^{-1}$ versus 0.1 s^{-1}). The η_i values are quite different than the bulk values at all annealing temperatures. We attribute the deviations of η_i from bulk to two probable causes. Besides the previously described the discrepancy in strain rates between the two techniques, an additional cause for deviation is related to the change in the Poisson's ratio for PS during the thermal wrinkling experiments at short times.

In all of our interpolations, we have assumed that the Poisson's ratio considered as an ideal rubbery network, i.e. an incompressible material ($\nu_i \approx 0.5$). It is valid to

assume that PS is incompressible at long annealing times for temperatures above T_g when the polymer can be approximated as a physically-entangled network of mobile chains. However, ν_i at short annealing times may be slightly less. More importantly, at these short times scales, ν_i is a time- and temperature-dependent quantity due to the viscoelastic response of PS. Therefore, slight changes in ν_i can lead to significant changes in η_i based on eq. (4).

Summary

Thermal wrinkling provides a new measurement approach for the viscoelastic properties of confined PS thin films above its glass transition temperature. We showed that by employing the equations established for theoretical buckling mechanics, it is possible to quantify the rubbery modulus and the shear viscosity of a PS thin film under confinement. This technique will provide a new measurement platform in quantifying the viscoelastic response of a variety of confined polymer systems.

Although this measurement technique is only demonstrated for amorphous PS, it is not limited to polymers with a glass transition. In general, as long as sufficient wrinkling strain is applied, this technique is capable of quantifying the viscoelastic properties of a variety of the polymer systems that under other forms of phase transitions, such as melting or order-disorder transitions.

Acknowledgements

The authors thank Sheng Lin-Gibson for the bulk rheology measurements and JunYoung Chung for insightful discussions. E.P.C. and K.A.P. acknowledge the NIST/National Research Council Postdoctoral Fellowship Program for funding.

Official contribution of the National Institute of Standards and Technology; not subject to copyright in the United States. Reported data error bars and value uncertainties represent one standard deviation as the estimated standard uncertainty of the measurements.

^{††} The equipment and instruments or materials are identified in the paper in order to adequately specify the experimental details. Such identification does not imply recommendation by NIST, nor does it imply the materials are necessarily the best available for the purpose.

Figures

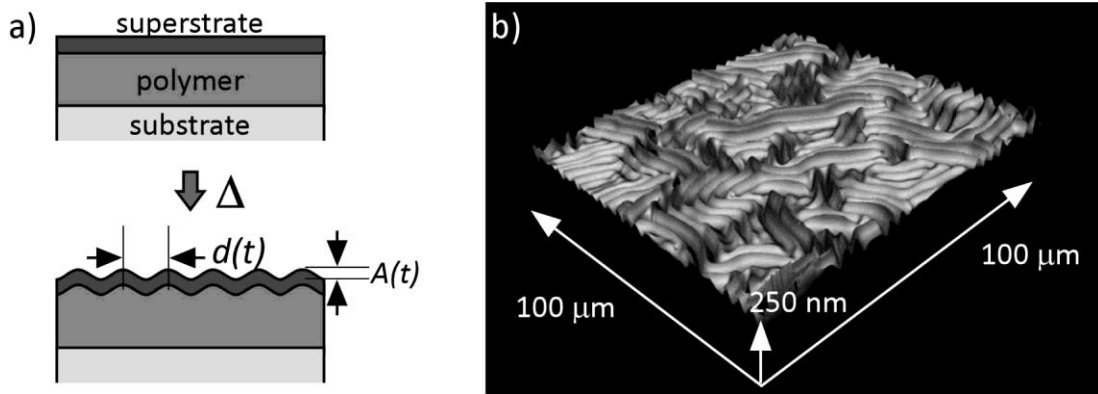


Figure 1. a) Schematic of the thermal wrinkling process that occurs when a polymer film confined by both a superstrate and substrate is heated to an elevated temperature. b) Optical profile image of a representative thermally-wrinkled surface illustrating the isotropic pattern characterized by defined wrinkle wavelength and amplitude.

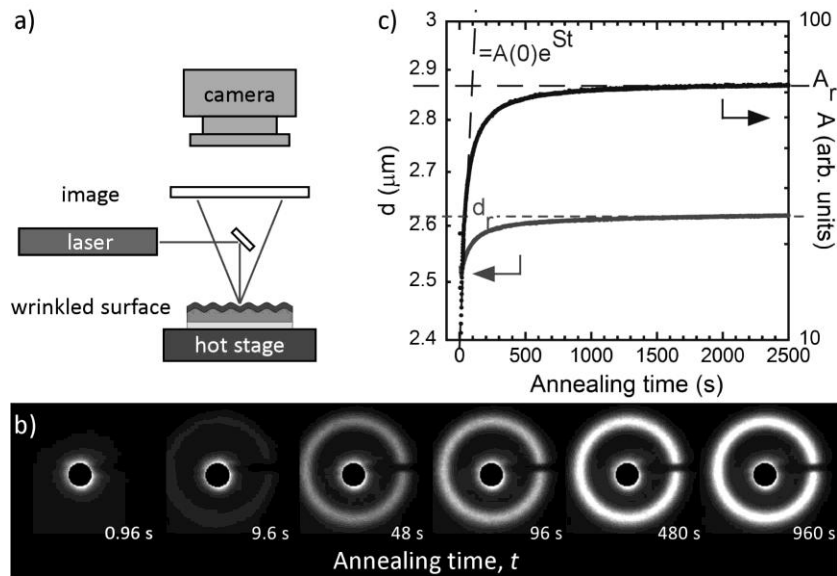


Figure 2. Experimental approach to measure the kinetics of the thermal wrinkling process. a) Schematic of the custom-built SALS instrument used to capture the wrinkling morphology in reciprocal space. b) Representative time-evolved scattering pattern as captured by SALS for the PS thin film at $125\ ^\circ\text{C}$. c) The corresponding time-evolved wrinkle wavelength (d) and amplitude (A). Figure reproduced by permission of The Royal Society of Chemistry.

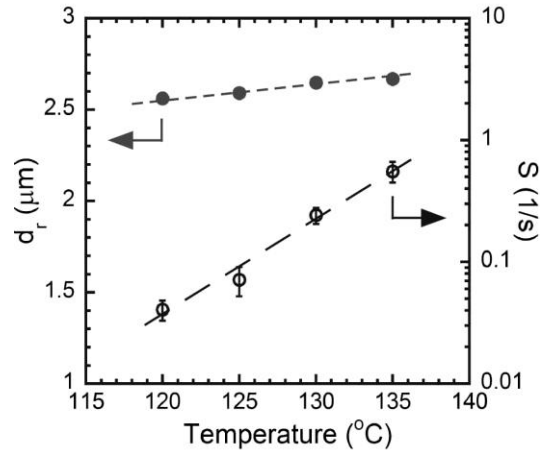


Figure 3. Changes in the long-time wrinkle wavelength (d_r) and short-time growth rate (S) as a function of annealing temperature. Figure reproduced by permission of The Royal Society of Chemistry.

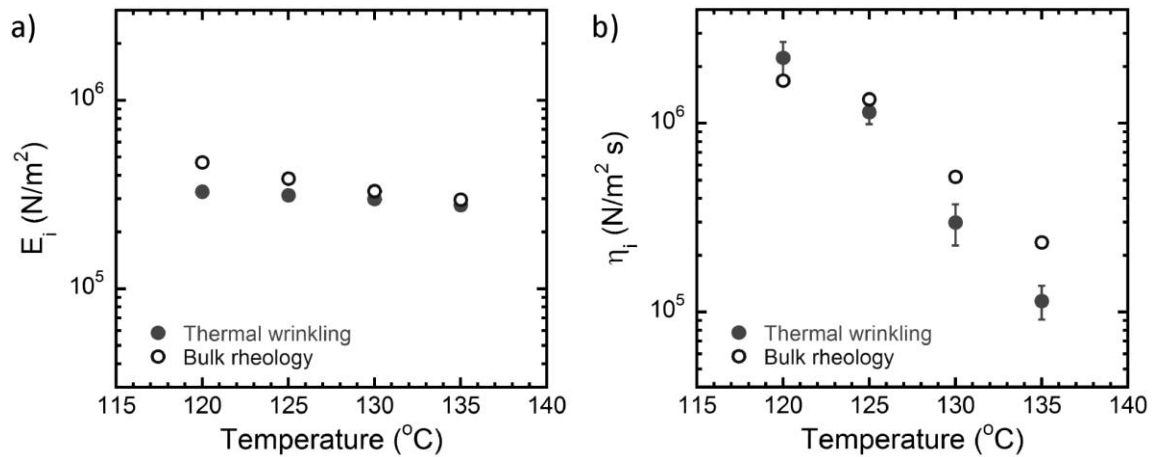


Figure 4. a) Changes in the rubbery modulus ($E_{i,r}$) as a function of annealing temperature and comparison with bulk rheology. b) Changes in the shear viscosity (η_i) as a function of annealing temperature and comparison with bulk rheology. Figure reproduced by permission of The Royal Society of Chemistry.

References

1. Stafford, C. M.; Vogt, B. D.; Harrison, C. M.; Julthongpiput, D.; Huang, R. *Macromolecules* 2006, *39*, 5095-5099.
2. Torres, J. M.; Stafford, C. M.; Vogt, B. D. *ACS Nano* 2009, *3*, 2677-2685.
3. Chan, E. P.; Page, K. A.; Im, S. H.; Patton, D. L.; Huang, R.; Stafford, C. M. *Soft Matter* 2009, *5*, 4638-4641.
4. Yoo, P. J.; Suh, K. Y.; Park, S. Y.; Lee, H. H. *Adv. Mater.* 2002, *14*, 1383-1387.
5. Okayasu, T.; Zhang, H.-L.; Bucknall, D. G.; Briggs, G. A. D. *Adv. Funct. Mater.* 2004, *14*, 1081-1088.
6. Kim, J.; Lee, H. H. *J. Polym. Sci., Part B: Polym. Phys.* 2001, *39*, 1122-1128.
7. Wallace, W. E.; van Zanten, J. H.; Wu, W. L. *Phys. Rev. E* 1995, *52*, R3329-R3332.